How does an Amorphous Surface Influence Molecular Binding? - Ovocleidin-17 and Amorphous Calcium Carbonate

SCHOLARONE™
Manuscripts

ARTICLE TYPE

How does an Amorphous Surface Influence Molecular Binding? - Ovocleidin-17 and Amorphous Calcium Carbonate†

Colin L Freeman,[a] **John H Harding,**[a] **David Quigley,**[b,c] **and P. Mark Rodger**[c,d]

Atomistic molecular dynamics simulations of dehydrated amorphous calcium carbonate interacting with the protein Ovocleidin-17 are presented. These simulations demonstrate that the amorphisation of the calcium carbonate surface removes water structure from the surface. This reduction of structure allows the protein to bind with many residues, unlike on crystalline surfaces where binding is strongest when only a few residues are attached to the surface. Basic residues are observed to dominate the binding interactions. The implications for protein control over crystallisation are discussed.

1 Introduction

Biomineralisation continues to fascinate and challenge our understanding of crystal growth and nucleation. The amazing structures produced by nature, such as nacre and the sea urchin spine[?]), require a level of control that is generally beyond anything that we can reproduce in a laboratory. Elucidating the role of biomolecules in this control is vital.

There are potentially many different stages in crystal growth and the processes employed by biomineral systems remains a much debated subject. The classical view of ions forming a nucleus in solution is now combined with, or challenged by, aggregation type models involving cluster formation[?,?], polymer-induced liquid phases[?], amorphous precursors[?] and spinodal phase separation[?]. In many cases of calcite formation the amorphous calcium carbonate (ACC) phase is seen before crystallisation. ACC exists in two different phases[?]: a stable phase with a high level of water content ($\sim$50% or greater) which is found in living organisms[?]; and a transient phase (with a low level of water content) that undergoes a rapid transition to calcite or another $CaCO_3$ polymorph. Debate continues in the literature as to the role of ACC phases in the crystallisation process with observations of crystallisation occurring within the amorphous phase[?] or potentially at the ACC/water interface while in other cases the ACC may have no major controlling function[?]. Calcite growth is expected to occur in regions with higher local concentrations of Ca and CO_3 ions but the major debate remains concerned with the structure/phase of this region. Therefore, to understand the role of biomolecules in stimulating and influencing crystal growth it is valuable to examine the interactions between biomolecules and ACC.

For a recent review of the science of eggshells we would refer the reader to Hincke *et al*[?]. The Ovocleidin-17 (OC-17) protein is found only in the ovaries of hens and is thought to play a major part in controlling eggshell production. It is an ideal candidate to examine as its sequence and crystal structure have been reported[?,?,?] and a range of studies has been performed on its function within the ovaries and during crystal formation[?,?,?,?,?]. These studies have demonstrated that this protein (and peptide derivatives of it) can influence calcite formation in vitro[?,?]. Our own computer simulations[?] demonstrated that the presence of OC-17 on ACC nanoparticles altered the free energy hypersurface of the particle - removing the free energy barrier between ACC and calcite. The simulations also showed that for a 300 formula unit nanoparticle, the protein bound far more strongly to the nanoparticle when the nanoparticle was amorphous rather than crystalline. Taken together this evidence implies that the protein may be able to bind to ACC and stimulate its conversion to calcite and then detach - effectively operating as a catalyst. The promotion of crystallisation seems a plausible function for OC-17 given that it is found in high concentrations in the mamilary caps of eggshells, which is where crystallisation begins[?,?]. We

[a] *Department of Materials Science and Engineering, Sir Robert Hadfield Building, Mappin Street, Sheffield, UK. Fax: +44 (0)114 2225943; Tel: +44 (0)114 2225965; E-mail: c.l.freeman@shef.ac.uk*
[b] *Department of Physics, University of Warwick, Gibbet Hill Road, Coventry, UK*
[c] *Centre for Scientific Computing, University of Warwick, Gibbet Hill Road, Coventry, UK*
[d] *Department of Chemistry, University of Warwick, Library Road, Coventry, UK*
‡ Additional footnotes to the title and authors can be included *e.g.* 'Present address:' or 'These authors contributed equally to this work' as above using the symbols: ‡, §, and ¶. Please place the appropriate symbol next to the author's name and include a \footnotetext entry in the the correct place in the list.

have continued our studies on OC-17 by examining the protein binding to the {10.4} and terraced surfaces of calcite and noted that the molecule is a strong binder on these surfaces when it is able to penetrate the surface water structure[?][?][?]. The obvious remaining question is to examine the binding of OC-17 on amorphous surfaces. Our simulations on crystallisation imply that a stronger binding mechanism should be present for ACC than is seen for the crystalline surfaces. Here we present molecular dynamics (MD) simulations of OC-17 interacting with a surface of anhydrous ACC. We discuss the binding mechanisms and their differences with those of crystalline surfaces.

2 Methods

All the simulations described in this paper were performed with classical molecular dynamics in the DL_POLY 3.09[?] code. Periodic boundary conditions were applied in all three dimensions with an ACC slab effectively separated from its periodic image by a slab of water in the Z-direction. A timestep of 1 fs was used along with the NVT Nose-Hoover thermostat (relaxation time 0.1 fs). The forcefield description of OC-17 was that of the general united atom AMBER model[?][*] *and the structure was taken from ref.*[?], while the calcium carbonate was described with *the rigid ion nonpolarisable* potentials of Pavese *et al*[?][?] and the water was modelled as TIP3P[?]. Newer forcefields have been developed for modelling calcium carbonate e.g.[?] but a recent review[?] has demonstrated that the Pavese model generates a more reliable surface structure for water on calcium carbonate which is the key parameter for our simulations. Using the Pavese potential also maintains consistency with our previous simulations of OC-17 which is important for comparison. Cross-terms between the protein/water and the calcium carbonate were as reported in our previous work[?][?][?].

The ACC surface was generated from the {10.4} slab of calcite generated for previous simulations[?]. This slab contained 4800 $CaCO_3$ formula units consisting of ten layers and measuring 100.6 Å and 97.5 Å in the x and y respectively. This slab was heated in vacuum from 300 K to 3000 K in 100 ps steps of 300 K and then held at 3000 K for 5.0 ns. Quenching of the slab was then performed to return the slab to 310 K. This was achieved by running a series of 100 ps simulations each

300 K cooler than the previous simulation until the temperature was returned to 310 K. Analysis of the radial distribution function (RDF) for the slab demonstrated that the slab was amorphous (see supplementary information Figure 1).

The construction of potential binding configurations followed an identical methodology to our previous study of OC-17 binding on the {10.4} surface[?] and the reader is referred to this reference for full details. Briefly, the protein was placed 8 Å above the ACC slab in 64 different orientations and at 16 different positions relative to the surface plane. The resulting 1024 configurations were then used in 200 ps vacuum simulations. For each of the 16 positions the highest and lowest energy configurations were identified. *These were chosen to provide the widest range of potential binding motifs in the sampling.* These starting orientations/positions of the protein were then used for solvated simulations using 20500 water molecules generated in a random configuration with the packmol package[?]. These 24 simulations were then run for at least 2 ns and the lowest energy position was selected for running for the total simulation time.

As with previous simulations, where the surface water was found to control the proximity of the protein to surface, the protein was displaced perpendicularly from the surface to begin the simulations at two different distances from the surface (∼4 Å and ∼8 Å - close and distant binder). Unlike previous simulations, however, these two different starting configurations resulted in the same final binding configuration. The distant binder migrated towards the surface and finished the simulation at approximately the same separation from the surface with the same residues in contact with the surface as the close binder. The protein binding simulations were all performed at 310 K and were run until the average value of the configurational energy (∼-2.44 x 10^7 kJmol^{-1}) had converged which took ∼30 ns. This was judged to have occured when four simulations of 0.7 ns produced a configurational energy within ±20 kJmol^{-1} of each other *(see supplementary information Figure 4)*.

2.1 Analysis Methods

During the simulations it was observed that all the Cl$^-$ anions (added to counter the +7e charge of the protein) adsorbed at the ACC surface and two entered the ACC slab and became fully immersed within the slab. These Cl$^-$ ions all adsorbed to the opposite side of the slab from the OC-17, and so were not directly involved in the binding of the protein. The large concentration of negative charge (-7e) at the surface may encourage binding of the positive OC-17 although the ACC is likely to block out most of this effect and the large number of carbonate anions at the surface will generate a far stronger attraction.

In previous simulations with crystalline slabs of calcite the

---

[*] Newer forcefields are now available for protein systems but when these simulations were performed 2008-2009 these were not in place. It should be noted that the presence of 3 s-s bridges means the structure of this protein is highly stable and therefore not capable of large changes (as noted in our analysis) therefore these improvements in forcefields would not affect the main structure. The structure we observe is extremely close to the crystal one we have used for our starting structure. The side chains are generally in highly ionic environments and therefore the crucial part of their forcefield is their interaction with the inorganic crystal where we have extensively tested the derived forcefields.

Cl$^-$ anions did interact with the surface but no incorporation was observed. To estimate the influence of chloride ion adsorption completely into the slab two further calculations were performed. An additional Ca^{2+} was added to the ACC slab to give the slab an overall charge of +2e. The slab was then solvated with 20500 water molecules (but no protein was added). Two chloride anions were then added to the simulation box. In the first simulation these were added both approximately 1 Å above the surface and in the second they were placed within the slab. The simulations were run with the same parameters as listed in the previous section. Extracting the energy difference between the two simulations provides an estimate of the energy difference for chloride adsorption from the surface into the slab which we calculate to be $\sim$ -100 kJmol^{-1} per Cl anion. This correction was applied to the adsorption energy of the OC-17 to generate a better comparison with the adsorption simulations on the calcite surfaces.

Other analysis methods - including the normal density profile, Root-mean square displacement (RMSD), H-bonding† and water counting at the interface - were carried out in the same manner as reported in previous publications[?][?].

3 Results and Discussion

The final binding configuration of OC-17 on the ACC surface can be seen in Figure 1. The binding motifs are very different to those for the crystalline surfaces (see Table 1). Firstly a very large number of residues, fifteen in total, interact with the slab. Although some of the residues adsorb onto the slab surface, several of the residues actually enter the slab, becoming surrounded by the Calcium and carbonate ions. This occurs for three adjoining residues, numbers 84-86, a glycine, serine and arginine. The diffuse structure of the ACC slab also results in carbonate anions diffusing out of the slab into the solution. Several of these solvated carbonates interact with residues, as seen in Figure 1 and highlighted in Table 1 *and shown in detail in the supplementary information.* The coil regions of the protein are primarily responsible for the interactions with the slab and the helix regions are generally distant from the slab. The residues that bind to the ACC are frequently adjacent to each other in the sequence (e.g. 81-87). On the crystalline surfaces the steric hindrance of the protein backbone prevented adjoining residues and their R-groups from simultaneously interacting with the surface. The greater flexibility gained from the ACC surface allows these residues to fully interact, e.g. the guadinium ions of both arginines 108 and 109 interact with the surface. The ability of the protein to make favourable interactions with the ACC (i.e. polar and charged atoms with the ions) is a general feature of the residue binding. No residue in-

---

† Defined with a total deviation from a linear bond of $<30^\circ$ and a total length of 3.3 Å (Oxygen-Oxygen)

teracts with the ACC via only non-polar atoms and a total of nine positive residues (eight arginines and one lysine) are in contact. A maximum of six charged residues were seen on the crystalline surfaces at any given time. Only positive residues interact with the surface. This may be largely a feature of the geometry of binding: within the sequence of residues that have bound (81-112) the only acidic residue is aspartate (92).

Despite the large number of residues binding to the ACC slab, the protein undergoes little structural changes *during the simulation time of tens of ns.* An analysis of the 1-4 RMSD of the atoms within the backbone of the protein shows only five have changed to a degree greater than two standard deviations from their expected positions *(see the supplementary information Figure 2).* This occurs for residues 27-30 and 33-36. These two points reside at either end of the first α-helix in the protein and their small change appears to be due to better structural definition of the helix in the structure. The other changes are in 106-109. This involves a lysine and two arginine residues that are bound to the ACC and suggests a small deformation that aids the binding of these residues. The final two cases are at residues 1-4 which appears to be a small unravelling of the end of the protein chain and 117-120 which is at the end of a β sheet and appears to occur due to a further curving the backbone appearing that is indicative of the start of an α-helix, although no full helix is formed only the initial first turn. This may be the result of the small structural change at 106-109 which occurs a little before a disulphide bridge between Cys 113 and Cys 130. The bridge sits between two β sheets and therefore the extra turn may be required to maintain the order of these sheet elements as the bridge is too rigid to adjust. That any changes in the 1-4 RMSD are observed is a difference to all the other binding configurations on crystalline surfaces which exhibited no significant changes in structure. This suggests that the protein does adopt interactions with the amorphous surface that may be stronger than those with the crystalline surface and therefore lead to very small structural changes.

The adsorption energy, -977.1 kJmol^{-1}, is over two times larger than that of OC-17 on the {10.4} surface *(-422 kJmol^{-1})*, indicating that binding is stronger. It should be noted this is a configuration energy and not a free energy. We discuss the entropic implications of the binding later.

The Z-density (Figure 2) of the water at the ACC surface shows that the organised layered structure seen on crystalline calcite surfaces is not present. The water and slab demonstrate some degree of overlap and the interface is not sharply defined. As one moves away in a direction normal to the surface there are peaks and minima in the Z-density of the water, but these are small compared with the peaks observed on the {10.4} surface. Although the ions in the ACC slab are still attractive to the water due to their large charges, the disordered arrangement means that they impose little ordering on
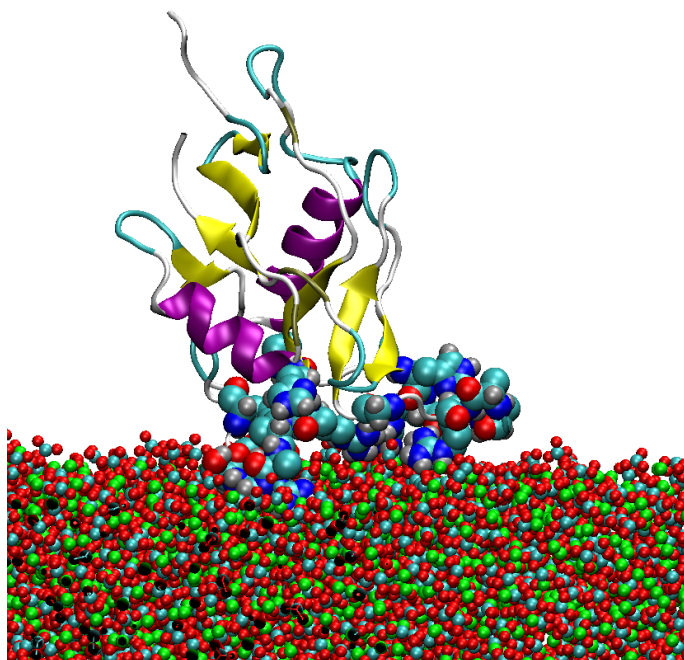
Fig. 1 Figure of OC-17 on the ACC surface.

Table 1 List of amino acid residues that interact with the ACC. Residue numerical sequence taken from ref.[?] . *Fraction of simulation time spent bound can be seen in supplementary information Figure 3.*

Close Binder Residue (number)	Interacting groups
arginine (81)	guandium ion - one carbonate out of surface in close proximity
proline (82)	backbone carbonyl
alanine (83)	backbone
glycine (84)	backbone - within the slab
serine (85)	alcohol and backbone amine - within slab
arginine (86)	guadinium ion - within slab
serine (87)	backbone amine and infrequent alcohol
arginine (89)	guadinium ion
arginine (97)	guadinium ion
arginine (103)	guadinium ion - one carbonate out of the slab
threonine (104)	alcohol group
lysine (106)	R-group amine
arginine (108)	guadinium ion
arginine (109)	guadinium ion - one carbonate out of the slab
arginine (112)	guadinium ion

the water. We can see this in part by counting the number of H-bonds for each water molecule on the surface. Table 2 lists the number of H-bonds between water molecules in particular water layers above (or separations from) the $CaCO_3$ slab with other water molecules in the same or different layers. At the {10.4} surface each water molecule in the 1st layer has an average of 1.03 H-bonds, while each one in the 2nd layer has an average of 0.9 H-bonds. In the amorphous system these values drop to 0.93 and 0.79 respectively [‡] This is because the water molecules at the amorphous surface are neither organised into clear layers moving perpendicularly away from the surface nor into a particular pattern in the plane of the surface. This organisation on the {10.4} surface forces the water molecules into particular positions which encourages the formation of H-bonds with each other.

The count of the number of water molecules at set separations from the Ca cations (Figure 3) demonstrates that fewer water molecules are present close to the interface with the amorphous surface compared with the crystalline {10.4} surface. In the region that the first two water layers are observed on the {10.4} surface there is a much greater density of water molecules (~4.6 molecules per 100 Å² at 3.5 Å separa-
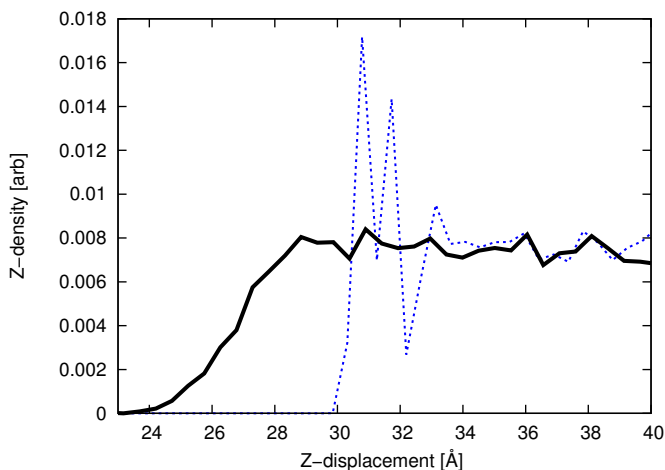

Fig. 2 Z-density for the Oxygen of the water molecules on the amorphous slab (solid black) and the {10.4} slab (dotted blue) with no OC-17 present.

[‡] The water layers in the case of ACC are not so clearly defined as for the crystalline surfaces. These have been judged by reference to Figures 3 and 4 which indicate a layering of water around Ca ions. These separations have been used to judge the layers at the ACC interface.

tion compared to ~2.0 molecules per 100 Å^2 on ACC). At the crystalline surface the water is organised into specific positions to maximise the interactions with the surface ions. This organised layer similarily imposes restrictions on the second layer of water due to the organisation of H-bonds between the molecules. Because the water is forced to adopt an ordered arrangement its density is increased above that of regular bulk water which is compensated for by the depleted region of water beyond the second layer. The disordered nature of amorphous surface imposes no such ordering on the water and therefore does not force it to increase density at the interface. So we see that the Z-density reaches a bulk like value at the interface and remains there in the ACC case (Figure 2) and that the total number of water molecules at the interface for ACC is smaller than for calcite (Figure 3). This is also demonstrated in Figure 4, which plots the number of water oxygens at a given separation from the surface Ca^{2+} cations. The first peak (representing the 1st and 2nd water layers) on the {10.4} surface is much larger than on the ACC surface. The second peaks have a similar maximum but the peak on the {10.4} surface is much narrower, suggesting a more localised region in which the water molecules are clustered. As one moves further from the surface the volume of water becomes the same for both the crystalline and ACC surfaces.

Note that the diffuse ACC interface with water allows water to reach small values of Z as the water can partially enter into the ACC slab. Despite this the total amount of water at the ACC interface is smaller than that of the {10.4} calcite surface. Only a small amount of water is diffusing into the ACC slab and in general the density of water at the ACC slab is not significantly larger than in the bulk unlike the calcite slab where the water density is significantly increased due to the organisation.

Table 3 Number of water molecules displaced by OC-17 at a separation of 5.0 Å between the Ca and the Oxygen (water).

Configuration	Total Number of water molecules
ACC	28.2
{10.4} - 1^a	16.1
{10.4} - 3^b	32.9

a Lowest energy binding configuration
b Highest energy binding configuration

We can calculate the number of water molecules displaced by examining the difference in water counts between the simulations with OC-17 present at the surface and absent at the surface (Table 3). This shows that 12 more water molecules are displaced on the ACC surface than for the lowest energy binding configuration on the {10.4} surface. The number is, however, lower than that observed for the highest energy bind-
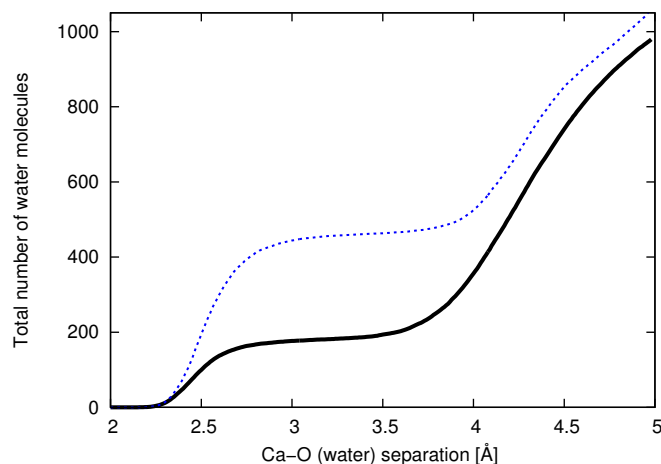

Fig. 3 Sum of the total number of water molecules at a given Ca-O (water) separation (i.e. total number of water molecules over the range 0-separation) for the ACC (solid black) and {10.4} (dotted blue) surfaces with no OC-17 present.
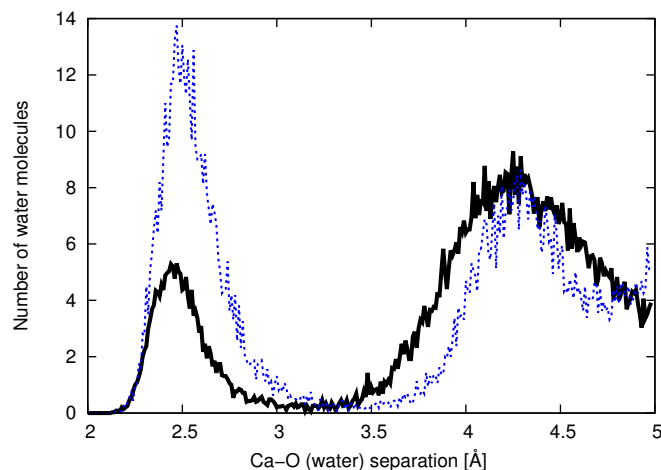

Fig. 4 Number of water molecules at a given Ca-O (water) separation for the ACC (solid black) and the {10.4} (dotted blue) surfaces with no OC-17 present.
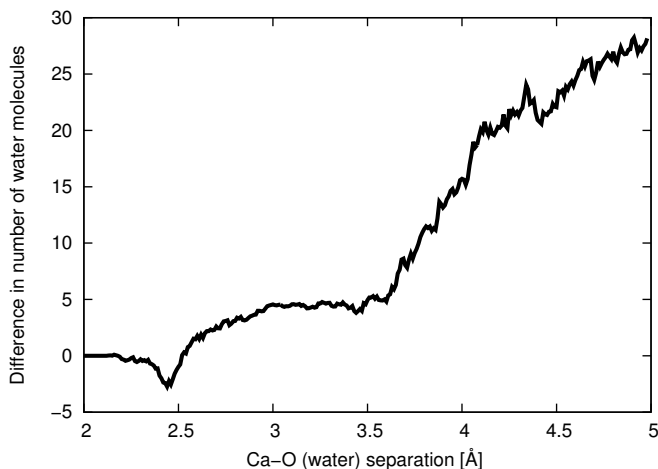
Fig. 5 The difference in the number of water molecules at a given separation from the Ca of the ACC surface for the system without OC-17 minus the system with OC-17 present.

ing configuration, on the {10.4} surface which displaced 4 more water molecules than the ACC configuration. This may seem surprising given the very large number of residues on the surface in the ACC configuration but there are two crucial differences. Firstly there is less water at the ACC surface than the {10.4} surface, which means that there is more space for the protein to enter. Secondly, the lack of water structuring means that the water on the ACC surface can readily move closer or further from the surface as it is pushed by the protein, whereas on the crystalline surface certain regions are energetically very unfavourable for the water. Figure 5 shows the difference between the number of water molecules at the ACC surface with and without the protein present. It can clearly be seen that more water is present very close to the surface ($\sim$ 2.4 Å) presumably because these molecules are pushed closer to the surface by the protein as it binds.

This result suggests that the protein binding on the ACC surface is far less regulated by the presence of the water than is the case for the crystalline surfaces. The water has a smaller binding energy on the ACC surface compared with the crystalline surfaces because it does not form the organised network which generates many inter water molecule H-bonds and a very favourable set of interactions with the ions in the surface. This means the water arrangement on the ACC surface is flexible so the protein can displace the water molecules with much more ease. The protein is also able to maximise its interactions with the surface since the surface is more deformable so the average interactions between each residue and the surface are probably stronger than for a crystalline surface where residues frequently are restricted in their interactions. We can presume that this result will be generic for many molecules and that binding will generally be stronger on ACC surfaces

compared with crystalline surfaces.

It should be noted the energetics we are discussing are configuration energies and not free energies. Calculating a free energy of binding for such a large molecule is would be computational extremely expensive. We can assume that the protein will loose entropy during the binding process but water displaced from the calcium carbonate slabs will gain entropy leading to potentially significant entropic contributions in the binding process. We have recently attempted to quantify these values for the {10.4} surface by estimating the entropy gain of water displaced from the surface ($\sim$6 Jmol^{-1}K^{-1}) into the bulk and applied this as a correction factor to our simulations[?]. The implication was that the extra entropy gained from displacing water molecules was not offset by the loss of interactions with the surface and we generated a value of -188 kJmol^{-1} as a *pseudo*-free energy of binding. On the amorphous surface the energy of this process would be expected to be very different. The water at the ACC surface is not ordered in the same way so we would expect a far smaller entropy gain for this water when displaced from the surface. This implies that the difference in free energy of binding between the calcite and ACC binding would be smaller than the difference in binding between the configurational energy alone. Even if we assume there is no entropy gain for displacing water from the ACC surface, however, we calculate the *pseudo*-free energy of binding as -755 kJmol^{-1} which is still much more negative than that on the {10.4} surface which suggests that binding on the amorphous is more favourable.

It is now interesting to consider the implications of this for OC-17 and eggshell formation. Our previous studies have suggested that OC-17 may accelerate the crystallisation of calcite and that the binding of OC-17 is stronger to the ACC nanoparticles than to the calcite nanoparticles. The results presented here indicate that OC-17 should bind more strongly to the ACC surface than to the crystalline {10.4} surface as observed with the nanoparticles. OC-17 does seem to have particular features that may enhance the difference in binding between the ACC and crystalline surfaces. Firstly, OC-17 is structurally rigid. The three disulphide bridges hold the globular structure in place and prevent any significant structural changes during binding. This largely limits binding to only the two loop regions of the protein which have some flexibility. Flexibility seems to be important for a molecule to maximise its interactions with a crystalline surface as this ensures that the strongly interacting functional groups are able to get into contact with the surface. Therefore the restrictions on the flexibility of OC-17 suggest that its binding on crystalline surfaces could be limited. Secondly, we also noted in previous studies that adjoining residues in the sequence were often unable to bind to crystalline surfaces as the structural positioning means that alternating residues would be pointing away from the surface. On the ACC surface this problem is largely re-

moved as the surface can accommodate this conformational restriction. In the loop regions of OC-17 we see several sections of charged residues which interact strongly with the ACC surface where the residues are adjoining (residues 81-87, 103-104 and 108-109), these regions do not interact as strongly with the crystalline surfaces as they do with the ACC surface (e.g. only 83, 85, 86 and 89 are seen bound to the {10.4} surface).

4 Conclusions

We have conducted MD simulations of the protein Ovocleidin-17 interacting with a slab of ACC. The simulations have identified a far larger number of basic and neutral residues interacting with the ACC than was observed with crystalline calcite surfaces. The diffuse interface between the ACC slab and the solvent allows the protein to become more immersed within the slab, which strengthens the protein-surface interactions. The lack of structured water at the ACC interface enables the protein to displace water with less energetic penalty than seen on crystalline surfaces, which also favours greater binding contact between the protein and ACC. Our simulations suggest that OC-17 is able to generate strong interactions with the amorphous surface in agreement to simulations on nanoparticles.

5 Acknowledgements

Notes and references

S. Weiner, L. Addadi and H. Wagner, *Materials Science & Engineering C-Biomimetic and Supramolecular Systems*, 2000, **11**, 1–8.

D. Gebauer, A. Voelkel and H. Coelfen, *Science*, 2008, **322**, 1819–1822.

R. Demichelis, P. Raiteri, J. D. Gale, D. Quigley and D. Gebauer, *Nature Communications*, 2011, **2**,.

L. B. Gower, *Chemical Reviews*, 2008, **108**, 4551–4627.

E. M. Pouget, P. H. H. Bomans, J. A. C. M. Goos, P. M. Frederik, G. de With and N. A. J. M. Sommerdijk, *Science*, 2009, **323**, 1455–1458.

A. F. Wallace, L. O. Hedges, A. Fernandez-Martinez, P. Raiteri, J. D. Gale, G. A. Waychunas, S. Whitelam, J. F. Banfield and J. J. De Yoreo, *Science*, 2013, **341**, 885–889.

L. Addadi, S. Raz and S. Weiner, *Advanced Materials*, 2003, **15**, 959–970.

Y. U. T. Gong, C. E. Killian, I. C. Olson, N. P. Appathurai, A. L. Amasino, M. C. Martin, L. J. Holt, F. H. Wilt and P. U. P. A. Gilbert, *Proceedings of the National Academy of Sciences of the United States of America*, 2012, **109**, 6088–6093.

Q. Hu, M. H. Nielsen, C. L. Freeman, L. M. Hamm, J. Tao, J. R. I. Lee, T. Y. J. Han, U. Becker, J. H. Harding, P. M. Dove and J. J. De Yoreo, *Faraday Discussions*, 2012, **159**, 509–523.

M. T. Hincke, Y. Nys, J. Gautron, K. Mann, A. B. Rodriguez-Navarro and M. D. McKee, *Frontiers in Bioscience-Landmark*, 2012, **17**, 1266–1280.

M. Hincke, C. Tsang, M. Courtney, V. Hill and R. Narbaitz, *Calcified Tissue Iinternational*, 1995, **56**, 578–583.

K. Mann and F. Siedler, *Biochemistry and Molecular Biology International*, 1999, **47**, 997–1007.

C. L. Freeman, J. H. Harding, D. Quigley and P. M. Rodger, *Journal of Physical Chemistry C*, 2011, **115**, 8175–8183.

J. Reyes-Grajeda, A. Moreno and A. Romero, *Journal of Biological Chemistry*, 2004, **279**, 40876–40881.

R. Lakshminarayanan, J. Joseph, R. Kini and S. Valiyaveettil, *Biomacromolecules*, 2005, **6**, 741–751.

L. Marín-García, B. Frontana-Uribe, J. Reyes-Grajeda, V. Stojanoff, H. Serrano-Posada and A. Moreno, *Crystal Growth and Design*, 2008, **8**, 1349–1435.

C. L. Freeman, J. H. Harding, D. Quigley and P. M. Rodger, *Angewandte Chemie-International Edition*, 2010, **49**, 5135–5137.

C. L. Freeman, J. H. Harding, D. Quigley and P. M. Rodger, *Physical Chemistry Chemical Physics*, 2012, **14**, 7287–7295.

C. L. Freeman and J. H. Harding, *Journal of Physical Chemistry C*, 2014, **118**, 1506–1514.

W. Smith and T. R. Forester, *Journal of Molecular Graphics*, 1996, **198/199**, 796–781.

W. Cornell, P. Cieplak, C. Bayly, I. Gould, K. Merz Jr., D. Ferguson, D. Spellmeyer, T. Fox, J. Caldwell and P. Kollman, *Journal of the American Chemical Society*, 1995, **117**, 5179–5197.

A. Pavese, M. Catti, G. D. Price and R. A. Jackson, *Physics and Chemistry of Minerals*, 1992, **19**, 80–87.

A. Pavese, M. Catti, S. C. Parker and A. Wall, *Physics and Chemistry of Minerals*, 1996, **23**, 89–93.

W. Jorgensen, J. Chandrasekhar, J. Madura, R. Impey and M. Klein, *Journal of Chemical Physics*, 1983, **79**, 926–935.

P. Raiteri and J. D. Gale, *Journal of the American Chemical Society*, 2010, **132**, 17623–17634.

P. Fenter, S. Kerisit, P. Raiteri and J. D. Gale, *Journal of Physical Chemistry C*, 2013, **117**, 5028–5042.

C. L. Freeman, J. H. Harding, D. C. Cooke, J. A. Elliot, J. S. Lardge and D. M. Duffy, *Journal of Physical Chemistry C*, 2007, **111**, 11943–11951.

C. L. Freeman, I. Asteriadis, M. Yang and J. H. Harding, *Journal of Physical Chemistry C*, 2009, **113**, 3666–3673.

J. Martinez and L. Martinez, *Journal of Computational Chemistry*, 2003, **24**, 819–825.

Table 2 Average number of H-bonds for water molecules within the first two layers on the amorphous and {10.4} surfaces. Note we only count donors for the H-bonds therefore the maximum number of H-bonds expected for any water molecule is 2.0.

| Surface | Layer | H-bonds with layer | | | |
		1st	2nd	bulk	total
amorphous	1st	0.03 ± 0.02	0.89 ± 0.06	0.01 ± 0.01	0.93 ± 0.06
amorphous	2nd	0.12 ± 0.01	0.02 ± 0.01	0.66 ± 0.02	0.79 ± 0.02
{10.4}	1st	0.01 ± 0.01	1.02 ± 0.03	0.00 ± 0.001	1.03 ± 0.03
{10.4}	2nd	0.52 ± 0.02	0.02 ± 0.01	0.36 ± 0.01	0.90 ± 0.02